DEVELOPMENT OF FABRY-PEROT INTERFEROMETERS
FOR AIRGLOW OBSERVATIONS

Mamoru Ishii[1], Shoichi Okano[2], Eiichi Sagawa[3], Shin'ichi Watari[1],
Hirotaka Mori[1], Iwao Iwamoto[1] and Yasuhiro Murayama[1]

[1]*Communications Research Laboratory, 2–1, Nukui-kitamachi 4-chome, Koganei-shi, Tokyo 184*
[2]*National Institute of Polar Research, 9–10, Kaga 1-chome, Itabashi-ku, Tokyo 173*
[3]*Hiraiso Solar Terrestrial Research Center, Communications Research Laboratory,
3601, Isozaki-cho, Hitachinaka 311–12*

Abstract: We are developing an all-sky and a scanning Fabry-Perot interferometer for studying the dynamics of the thermosphere and the mesosphere in the polar region. Our instruments have three unique features useful for airglow observation; (1) Each instrument can obtain interference fringes at two different wavelengths at a time using a dichroic mirror, (2) The instruments can observe very weak airglow with the aid of a photon counting imager, (3) When operated simultaneously, the all-sky and the scanning Fabry-Perot interferometer can observe vertical winds in addition to two-dimensional atmospheric motions. We have made two test observations at the Zao observatory, Tohoku University in 1994, and at the Shigaraki observatory, Kyoto University in 1995.

1. Introduction

Optical observation can be a very powerful approach for obtaining information regarding the dynamics of the lower thermosphere and the mesosphere. Radar observation can derive the altitude profile of wind and temperature for electrons and ions directly. However, some assumptions are inevitable to infer the dynamics of the neutral atmosphere (*e.g.*, Brekke *et al.*, 1974). The Fabry-Perot interferometer (FPI) has an advantage of measuring the velocity and temperature of neutral atmosphere rather directly in the thermosphere and the mesosphere from the Doppler shift and broadening of airglow emission lines.

As study progresses regarding the interaction between lower thermosphere and mesosphere, we are becoming more aware of the importance of studying vertical winds and the small-scale structure of the wind system. Especially for the polar region, a number of scientists are paying attention to the energy interactions between auroral activities and the thermosphere. Recently, lots of studies have been published on vertical winds (Conde and Dyson, 1995; Aruliah and Rees, 1995; Smith and Hernandez, 1995; Sipler *et al.*, 1995; Price *et al.*, 1995; Laakso *et al.*, 1995). Vertical winds play a significant role in determining the composition, large-scale circulation and energy balance of the upper atmosphere. Yet, in many

studies by both theoreticians and experimentalists, the vertical wind component is assumed to be zero. Determining the validity of this assumption has become a very important issue.

Communications Research Laboratory has undertaken a research project on the polar mesospheric region in cooperation with the University of Alaska, Fairbanks, using various instruments (hereafter it will be called Alaska project). As a part of this project, we are in charge of developing two types of Fabry-Perot interferometer, *e.g.*, a scanning type and an all-sky type.

The scanning FPI has been built to observe vertical winds in the thermosphere and the mesosphere. Using it along with the all-sky FPI, we can obtain two-dimensional a wind and temperature structure. In addition, it is possible to infer the wind and temperature at two different altitudes, because each instrument can observe the airglow of two different wavelengths simultaneously. Until now there are few opportunities to observe both vertical winds and two-dimensional distribution of horizontal winds simultaneously. We hope that our instruments will give us important information about vertical winds from the simultaneous use of the two FPIs. This paper presents the instrumentation of two types of FPI and future observation plans.

2. Instrumentation

We have developed two types of FPI. One is a conventional FPI which can scan the sky with a narrow field of view (1.4 deg. full angle). It can point to the desired portion in the sky using a moving mirror system. The other has a wide field of view (140 deg. full angle); it can perform two-dimensional observation of the airglow. Figure 1 is an external view of the scanning FPI (right side) and the all-sky FPI (left side).

Three marked aspects of our instruments should be mentioned for airglow observations; (1) Each instrument can observe the airglow at two different wavelengths simultaneously, using a dichroic mirror and two photo-detectors. (2) They can detect very weak airglow by deploying a photon counting imager (PCI) as a detector. (3) They can measure vertical component of atmospheric motion in addition to the two-dimensional distribution when used simultaneously.

The two instruments are identical except for their fore-optical systems. The core of each FPI is a 116-mm clear aperture, capacitance-stabilized Fabry-Perot etalon (Queensgate Instruments, Ltd.). The nominal etalon gap is 20.49 mm corresponding to free spectral range (FSR) of 0.00968 nm. It can be piezoelectrically scanned. The reflectivity of inner surface of the etalon (R) is measured to be $90 \pm 2.5\%$ in the wavelength region between 557.7 nm and 850.0 nm. The theoretical half width at half-maximum is 0.38–0.65 pm. Figures 2a and b are schematic diagrams of the scanning FPI and the all-sky FPI, respectively. The beam passing through the etalons is separated by a dichroic mirror. The light with a wavelength longer than 600.0 nm is reflected by the dichroic mirror, and those shorter than this threshold passes through it. With this mirror, we can observe the airglow emissions

Fig. 1.   Exterior view of the scanning Fabry-Perot interferometer (right side) and the all-sky Fabry-Perot interferometer (left side).

at two different wavelengths, one at 557.7 nm and the other at either 630.0, 843.0, or 850.5 nm, using interference filters, simultaneously with each instrument. The wavelength of peak transmission and the full width at half-maximum (FWHM) of these filters are given in Table 1.

Photon Counting Imagers (PCIs, Hamamatsu Photonics Co., V5102UHX (S-20, S-25)) are employed to detect fringes of weak airglow emission. The PCI is a 3-stage proximity focused image intensifier with a phosphor screen output. The PCIs are cooled down to $-15°C$ with a Peltier refrigerator to reduce thermal noise. The enhanced fringe image is optically coupled to a CCD camera having 512 by 480 pixels. Video signal from the CCD camera is digitized with one-bit A-D converter to reduce thermal noises of PCI and CCD. The digitized video images (30 frames/ s) are accumulated in the image processor to produce an image data with a good signal-to-noise ratio. Accumulation time can be externally adjusted to the intensity
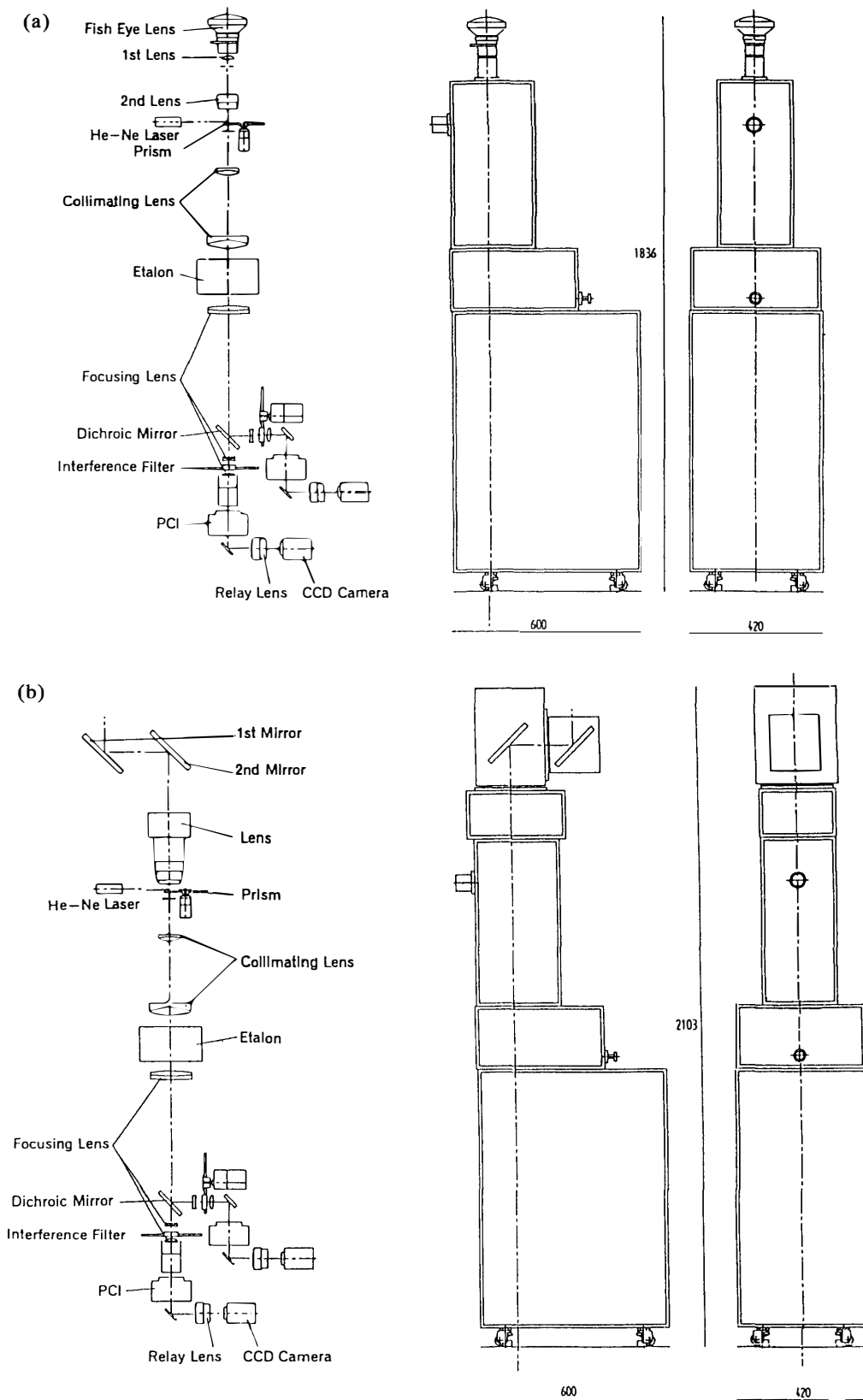
Fig. 2. Optical diagram of the Fabry-Perot interferometers: (a) all-sky Fabry-Perot interferometer; (b) scanning Fabry-Perot interferometer.

of incoming light. In addition to the accumulation time, data transfer between the image processor and computer and software control of the image processor require about 10 s for each image. This means that we can make observation almost continuously when strong airglow emission exists. Both instruments are controlled by separate UNIX workstations. These workstations are also used for storing data. Since the output data format is made similar in both data processing systems, almost all programs for observation and for analysis are compatible for both the scanning FPI and the all-sky FPI. Figure 3 is a system diagram of the scanning FPI. The system diagram of the all-sky FPI is almost the same. The instrument parameters of scanning and all-sky FPIs are summarized in Table 2.

Table 1.   The center wavelength and the full width at half-maximum (FWHM) of filters.

Scanning		All-sky	
Peak wavelength (nm)	FWHM (nm)	Peak wavelength (nm)	FWHM (nm)
557.521	2.0	557.700	1.9
630.841	2.7	630.664	2.6
843.034	1.0	843.134	1.0
850.496	1.0	850.636	1.1
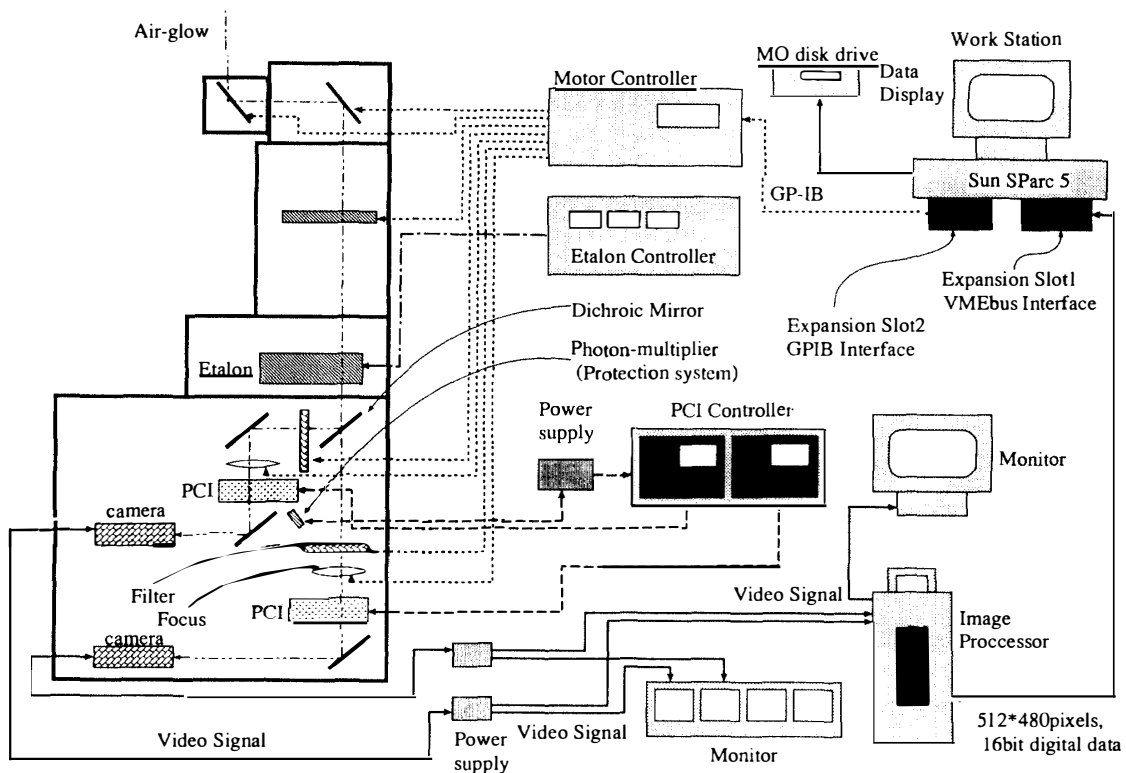
Fig. 3.   System diagram of the scanning Fabry-Perot interferometer. The system diagram of the all-sky FPI is almost the same.

Table 2. Summary of the instrument parameters of the Fabry-Perot interferometers.

Parameter		Value
Foreoptics		
Field of view	All-sky	Scanning
	140°	1.4°
Etalon (Queensgate Model ET116)		
Clear aperture		116 mm
Reflectivity (at 557.7–850.0 nm)		0.90±0.025
Theoretical reflective finesse		23.5–40.3
Nominal optical spacing		20.49 mm
PIH detector (Hamamatsu Model U5102UHX) (S-20, S-25)		
Collecting area		18 ϕmm
Resolution	S-20	20.21 line pairs/mm
	S-25	25.41 line pairs/mm
Amplification factor (photon counting mode)		10^7 fl/fc
Quantum efficiency	at 557.7 nm	10%
	at 630.0 nm	11%
	at 843.0 nm	4.7%
	at 850.5 nm	4.2%
Dark count (0°)	S-20	8.2 cps/mm²
	S-25	4.1 cps/mm²
CCD detector (Hamamatsu C3077-02)		
Imaging area	H	8.8 mm
	V	6.6 mm
Pixel number	H	768
	V	493
Pixel size	H	11.0 μm
	V	13.0 μm

3. Preliminary Observations

Preliminary observations have been carried out during four new moon periods until the end of December 1995. First, observation was made at the Zao observatory, Tohoku University from November 24 through December 10, 1994. The Zao observatory has facilities for optical observations. There are four observation hatches (two measuring 1.2 m by 1.2 m square and two 0.9 m by 0.9 m square) on the roof, and one of them (1.2 m by 1.2 m) was allocated for our instruments. Besides our instruments, Tohoku University's FPI and a Multicolor All-sky Imaging System (MAIS) are operated routinely.

During the above-mentioned period, airglow observation was made on nine nights. Since only one hatch is available, we shared it for the scanning FPI and the all-sky FPI during the observation period. Specifically, the scanning FPI was operated for six nights and the all-sky FPI for three nights. In this observation, it
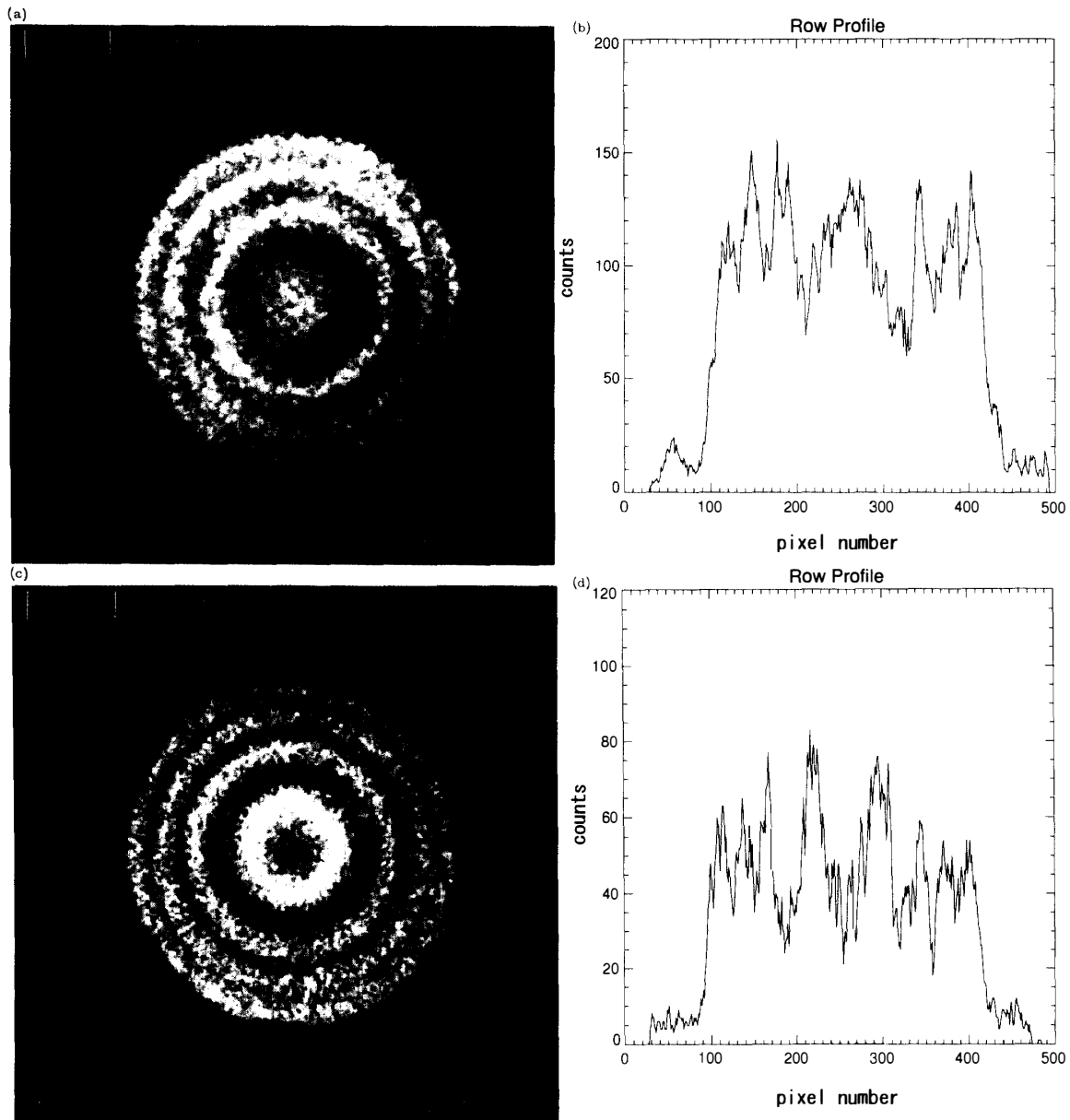
Fig. 4. (a) An example of fringe using the all-sky FPI with a 630.0 nm filter. The data were obtained between 2122:05 and 2127:39 on November 20, 1995. The image is given under 10000 times of accumulation of video image. (b) Horizontal cross-section of the fringe. (c) An example of fringe using the all-sky FPI with a 557.7 nm filter. The data were simultaneously obtained with the 630.0 nm data shown in (a). (d) Horizontal cross-section of the fringe.

was confirmed that our instruments have the capability that had been designed.

After the observation at Zao, the instruments were moved to the Shigaraki observatory, Kyoto University and observations were made for three new-moon periods. These observation periods were, September 13 through October 1, November 15 through 29, and December 15 through 29, 1995, respectively. Figure 4 shows an example of simultaneous observations of two fringes with different wavelengths and cross-sections of them. In this case, interference filters in A-ch and B-ch are

(a)

(b)
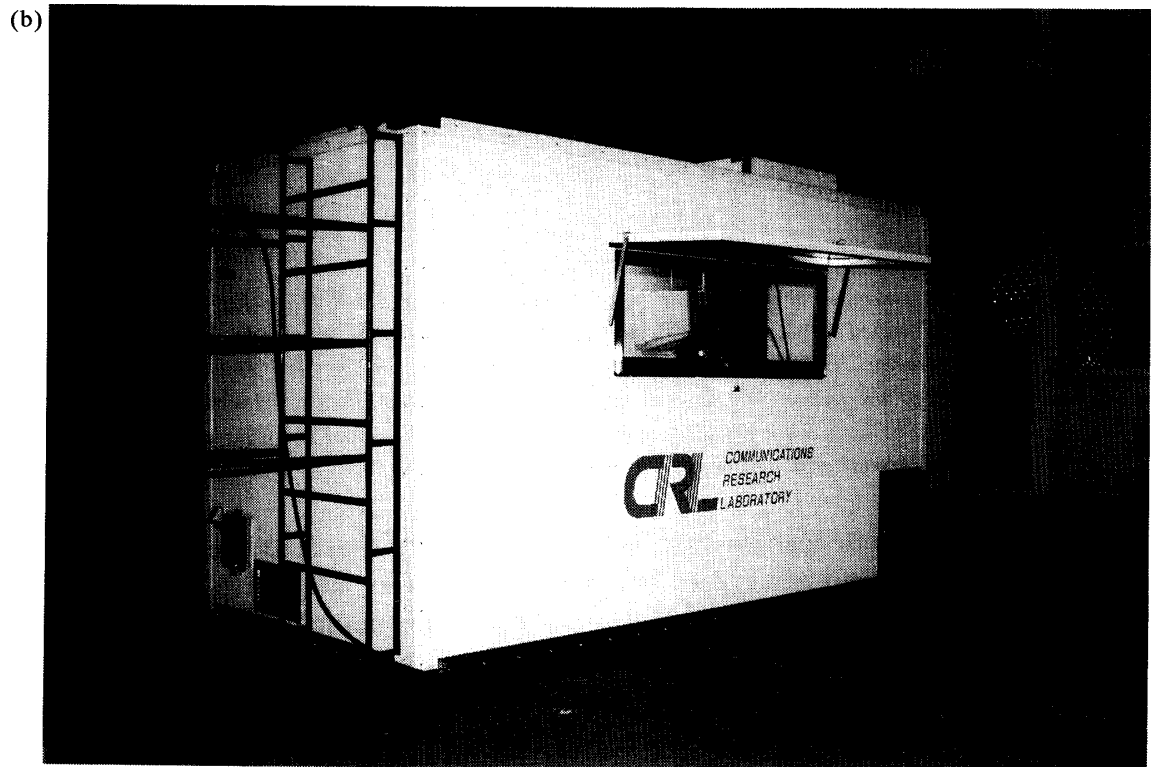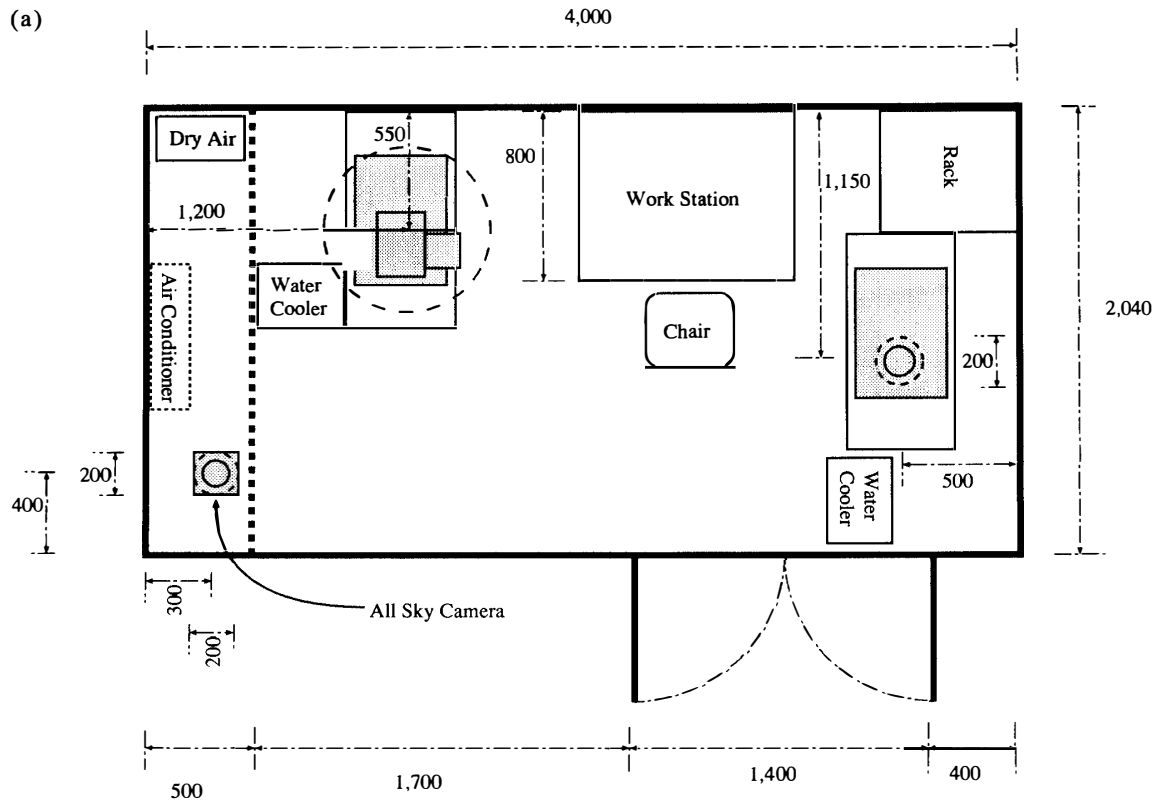
Fig. 5. *(a) Floor plan of the housing module for the FPIs. (b) Exterior view of this module.*

630.0 nm and 557.7 nm, respectively. This example was taken between 2122:05 and 2127:39 (a duration of 5 min 34 s) on November 20, 1995. The intensity of each photon spot recorded by CCD camera with electric potential between 0 and 2.0 V is converted into an integer from 0 to 255 in gray scale in the A-D converter. The threshold for digitizing is determined at 30 in these examples.

For these domestic observations, we prepared a housing module transportable by a truck. Figure 5 is a picture of the module and its plan view. With this module we can make observation at any site we want as far as electricity is available. In addition, it has three hatches on its roof for observation that make possible simultaneous operation of the scanning FPI and the all-sky FPI. The third hatch is for an all-sky CCD camera system which monitors existence of clouds and its locations two-dimensionally. The CCD camera has a fish-eye lens similar to that of the all-sky FPI for easy comparison between two images. The CCD camera is controlled by a PC and it takes an image every 90 s and image data are stored in the hard disk of the PC.

This module has a window with a shade which can make the module to a darkroom. An air conditioner installed in the module keeps the inside temperature at about 15 to 25°C.

During these observation periods, several other optical instruments were deployed by other groups and optical observations were made in cooperation with the MU radar (FUKAO et al., 1985a, b, 1990) at Shigaraki.

Tohoku University installed and operated the MAIS in the September and December periods for imaging airglow. A group of Shinsyu University installed and operated their sodium lidar for entire periods. A scanning photometer of INPE, Brazil was operated in September for OH rotational temperature measurements. In addition, an imaging observation of airglow was also made by Utah State University in November.

The present status of our data analysis is reported here. A program for determining wind velocities is still in progress. The center of a fringe is determined using a He-Ne laser as a calibration source for long-wavelength data and using a 557.7 nm discharge lamp (Resonance Ltd. Canada) for short-wavelength data. The fringe data are divided into 24 azimuthal sectors. After that, peak positions of a fringe along the 24 azimuthal directions are determined by fitting a Gaussian function to the fringe profile and the difference of the peak position from the wind velocity zero reference position is obtained (e.g., NAKAJIMA et al., 1995; NIIHARA, 1995). The most important issue we have to face is the way for determination of the wind velocity zero peak position. We have tried to use the fringe obtained with the 557.7 nm discharge lamp to determine such reference position. However, these data sets have insufficient signal-to-noise ratio for the analysis so far. We are still trying to suppress the background noise in such calibration data. A different approach for determination of the wind zero reference is to obtain fringes on fairly uniformly cloudy nights. We are also going to try this method in the near future.

4. Future Plans

Our instruments, the scanning FPI and the all-sky FPI, have been prepared for the Alaska project. They will be installed in the winter of 1997–1998. Before moving the instruments to Alaska, two observations are scheduled. The first is the observation of airglow simultaneously with the MF radar. Communications Research Laboratory has an MF radar in Yamagawa, Kyushu island (31.2°N, 130.6°E). This MF radar started operation in the end of August 1994. It is a pulse radar that uses a radio frequency of 1.955 MHz (153.5 m wavelength) and has a peak output power of 50 kW. The pulse is transmitted from one transmitter and reflected partially on the D layer of the ionosphere. Echos are received by three antennas. We can retrieve wind velocities at an altitude range of 80 to 100 km during the night with a temporal resolution of two minutes and a spatial resolution of 4 km (personal communication from K. IGARASHI, Communications Research Laboratory). Wind velocities in the same region can be obtained from the FPI observation of the OI 557.7 nm and OH 843.0 nm, 850.5 nm airglow. Such coordinated observations will be made in March, May, and August 1996. In August, we will take part in a campaign observation of the E region field-aligned irregularities (FAI) with the Sporadic E-layer (Sporadic-E Experiment over Kyushu (SEEK), coordinated by Prof. S. FUKAO, Kyoto University).

Next, the FPI instruments will be moved in Tromsø, Norway temporarily and coordinated observations will be carried out with the EISCAT radar. The EISCAT radar system has various observation modes (RISHBETH and EYKEN, 1993). For our observations a mode similar to CP-1, which measures several volumes distributed along the magnetic field line connected to Tromsø, will be used. The altitudes where we are going to measure three-component plasma velocities may be slightly different from those used in CP-1, depending on which emission line is to be used for determination of the neutral wind. The scanning FPI has a narrow field of view and it can measure the emissions from the similar volume as the EISCAT CP-1 type mode does.

The neutral wind that an FPI measures is the height averaged information and the method provides no altitude resolution. While the IS radar has sufficient altitudinal resolution of a few km, it requires some assumptions to derive the neutral wind from plasma movements. In the most popular method to deduce the neutral wind in the E-layer, the ion drift velocities are measured in the E-and F-layer. It is assumed that the electric field in the F-region is conserved along the magnetic field. The difference of the ion-drift velocity between E- and F-region is thought to come from neutral wind (*e.g.*, BREKKE *et al.*, 1974). In addition, collision frequency between ion and neutral is assumed from a model in many cases. It is not clear that these assumptions are appropriate even in geomagnetically disturbed condition. We hope that simultaneous observation of the FPI and the IS radar will give some insights to resolve their respective ambiguities.

Measurements of vertical component of neutral wind become the most impor-

tant topic for revealing the interaction between the upper and the lower thermosphere. The magnitude of vertical wind is generally thought to be far less than that of horizontal wind. However, several observation show that vertical winds up to 150 m/s exist in the high latitude regions, often in association with auroral Joule heating or sometimes those to auroral arcs (e.g., REES et al., 1984; CRICKMORE et al., 1991). The result shows that the vertical wind is not negligible in such cases.

One of the most advantageous point of our system is that the vertical and horizontal wind distribution can be observed simultaneously. The scanning FPI can detect vertical wind with fixing the elevation angle of mirror 90° with observing 2-dimensional distribution of neutral wind with the all-sky FPI. In general, vertical wind is assumed to zero for calculating horizontal wind. But in this way the horizontal wind distribution can be calculated using the observed vertical wind.

5. Conclusions

We are developing Fabry-Perot interferometers. One is a conventional Fabry-Perot interferometer with a narrow field of view; it can be pointed to the desired portion of the sky using a moving mirror system. The other is an all-sky Doppler imaging FPI; it can show the two-dimensional distribution of wind and temperature. In initial observations, we have confirmed that our FPI system has the high capability that we expected. Several simultaneous observations with the MU radar of Kyoto University at Shigaraki have been carried out. In the future, we will start simultaneous observations with the MF radar at Yamagawa observatory, Communications Research Laboratory. In winter 1997–1998, we will undertake a cooperative project with the EISCAT radar at Tromsø, Norway.

Acknowledgments

References

ARULIAH, A. L. and REES, R. (1995): The trouble with thermospheric vertical winds: Geomagnetic, seasonal and solar cycle dependence at high latitudes. J. Atmos. Terr. Phys., 57, 597–609.
BREKKE, A., DOUPNIK, J. R. and BANKS, P. M. (1974): Incoherent scatter measurements of E region conductivities and currents in the auroral zone. J. Geophys. Res., 79, 3773–3790.
CRICKMORE, R., DUDEREY, J. R. and RODGER, A. S. (1991): Vertical winds at the equatorward edge of the auroral oval. J. Atmos. Terr. Phys., 53, 485–492.
CONDE, M. and DYSON, P. L. (1995): Thermospheric vertical winds above Mawson, Antarctica. J.

Atmos. Terr. Phys., **57**, 589–596.

FUKAO, S., SATO, T., TSUDA, T., KATO, S., WAKASUGI, K. and MAKIHIRA, T. (1985a): The MU radar with an active phased array system 1. Antenna and power amplifiers. Radio Sci., **20**, 1155–1168.

FUKAO, S., TSUDA, T., SATO, T., KATO, S., WAKASUGI, K. and MAKIHIRA, T. (1985b): The MU radar with an active phased array system 2. In-house equipment. Radio Sci., **20**, 1169–1176.

FUKAO, S., SATO, T., TSUDA, T., YAMAMOTO, M., YAMANAKA, M. D. and KATO, S. (1990): MU radar: New capabilities and system calibrations. Radio Sci., **25**, 477–485.

LAAKSO, H., AGGSON, T. L., HERRERO, F. A., PRAFF, R. F. and HANSON, W. B. (1995): Vertical neutral wind in the equatorial *F*-region deduced from electric field and ion density measurements. J. Atmos. Terr. Phys., **57**, 645–651.

MORI, H., ITABE, T., MASUKO, H. and IGARASHI, K. (1995): International joint project for observation of the earth's environment at Alaska. J. Commun. Res. Lab., **42**, 255–263.

NAKAJIMA, H., OKANO, S., FUKUNISHI, H. and ONO, T. (1995): Observations of thermospheric wind velocities and temperatures by the use of a Fabry-Perot Doppler imaging system at Syowa Station, Antarctica. Appl. Opt., **34**, 8382–8395.

NIIHARA, Y. (1995): Chûido Kabu Netsuken-fû no Doppler-imaging Kansoku. Master thesis, Tohoku University (in Japanese).

PRICE, G. D., SMITH, R. W. and HERNANDEZ, G. (1995): Simultaneous measurements of large vertical winds in the upper and lower thermosphere. J. Atmos. Terr. Phys., **57**, 631–643.

REES, D., SMITH, R. W., CHARLETON, P. J., MCCORMAC, F. G., LLOYD, N. and STEEN, A. (1984): The generation of vertical thermospheric winds and gravity waves at auroral latitudes–I. Observations of vertical winds. Planet. Space Sci., **32**, 667–684.

RISHBETH, H. and VAN EYKEN, A. P. (1993): EISCAT: Early history and the first ten years of operation. J. Atmos. Terr. Phys., **55**, 525–542.

SIPLER, D. P., BIONDI, M. A. and ZIPF, M. E. (1995): Vertical winds in the midlatitude thermosphere from Fabry-Perot interferometer measurements. J. Atmos. Terr. Phys., **57**, 621–629.

SMITH, R. W. and HERNANDEZ, G. (1995): Vertical winds in the thermosphere within the polar cap. J. Atmos. Terr. Phys., **57**, 611–620.